

## Supporting Information

### **Teaching copolymerization catalysis to metal-organic frameworks by confining molecular catalysts in lattices**

Chao-Yu Chiu,<sup>a</sup> Chia-Her Lin,<sup>b</sup> Pei-Wen Wu,<sup>c</sup> Zhuorigebatu Tegudeer,<sup>d</sup> Chen-Yen Tsai,<sup>\*c</sup> and Wen-Yang Gao<sup>\*d</sup>

<sup>a</sup>*Department of Chemistry, National Taiwan Normal University, Taipei 24449, Taiwan.*

<sup>b</sup>*Department of Chemistry, National Tsing Hua University, Hsinchu 300044, Taiwan.*

<sup>c</sup>*Department of Chemistry and Biochemistry, National Chung Cheng University, Chiayi 62102, Taiwan. E-mail: chyetsai@ccu.edu.tw*

<sup>d</sup>*Department of Chemistry and Biochemistry, and Nanoscale & Quantum Phenomena Institute, Ohio University, Athens, Ohio 45701, United States. E-mail: gaow@ohio.edu*

## Table of Contents

A. General Considerations	S3
B. Synthesis and Characterization	S4
C. Supporting Data	S5
D. References	S35

## A. General Considerations

**Materials** Solvents were obtained as ACS reagent grade. Unless otherwise noted, all chemicals and solvents were used as received. Zirconyl chloride octahydrate, 1,3,6,8-tetrakis(*p*-benzoic acid)pyrene (H<sub>4</sub>TBAPy), *N,N*-dimethylformamide (DMF), benzene-*d*<sub>6</sub> (C<sub>6</sub>D<sub>6</sub>), and dimethyl sulfoxide-*d*<sub>6</sub> (DMSO-*d*<sub>6</sub>) were purchased from Sigma-Aldrich. Dichloromethane and methanol were obtained from Millipore. Ethanol was obtained from TEIDA. Toluene was obtained from J. T. Baker. Potassium bromide and trifluoroacetic acid (TFA) were obtained from Alfa Aesar. Hydrochloric acid (37% aq.) was obtained from Honeywell. Benzoic acid was obtained from SHOWA. Tetrabutylammonium bromide (TBAB) was obtained from Acros Organics. 4-Vinyl-1-cyclohexene 1,2-epoxide (VCHO), cyclohexene oxide (CHO), propene oxide (PO) and cyclopentene oxide (CPO) were purified by distillation over calcium hydride (CaH<sub>2</sub>) at least three times prior to use. Phthalic anhydride (PA) was purchased from Sigma Aldrich (98% purity) and purified by subliming three times. The NNO-2Ni molecular complex was synthesized according to literature.<sup>1</sup> UHP-grade (99.999% purity) N<sub>2</sub> and He used in gas adsorption measurements were obtained from Min Yang. All reactions were carried out under an ambient atmosphere unless otherwise noted.

**Characterization Details** NMR spectra were recorded on a Varian MR 400. Spectra were referenced against residual proton solvent resonance: C<sub>6</sub>D<sub>6</sub> (7.16 ppm, <sup>1</sup>H) and CDCl<sub>3</sub> (7.26 ppm, <sup>1</sup>H).<sup>2</sup> Powder X-ray diffraction (PXRD) pattern was measured with a Bruker D8 ADVANCE ECO using CuK $\alpha$  radiation  $\lambda$ = 1.54178 Å. High resolution scanning electron microscopy (HR-SEM, JEOL JEM-7600F) was used to investigate the morphology of MOF samples. Infrared spectra were recorded on an FT/IR-4200 spectrometer from Jasco Inc., Japan. Inductively coupled plasma optical emission spectroscopy (ICP-OES) was carried out using an Agilent 5110. The samples were dissolved in respective solvents by shaking, then dissolved in 50 mL of 5% nitric acid solution, and filtered prior to analysis. The concentration was adjusted according to the first scan. X-ray photoelectron spectroscopy (XPS) was carried out on a Thermo Scientific VG-Sigma Probe (Al K $\alpha$ , 1486.6 eV) and data were calibrated using carbon 1s signal at 284.8 eV. N<sub>2</sub> adsorption isotherms at 77 K were collected using a Micromeritics 3Flex. The samples were activated under high vacuum at 100 °C for 1000 min prior to the gas adsorption analysis. Gel permeation chromatography (GPC) measurements were performed on a Jasco PU-2080 plus system equipped with a RI-2031 detector using THF (HPLC grade) as an eluent (flow rate 1.0 ml/min at 40 °C). All X-ray absorption experiments were carried out at the National Synchrotron Radiation Research Center (NSRRC) located at Hsinchu, Taiwan. The matrix-assisted laser desorption ionization-time of flight mass spectrometry (MALDI-TOF MS) data were recorded using a Bruker UltrafleXtreme MALDI-TOF/TOF mass spectrometer.

## **B. Synthesis and Characterization**

### **Synthesis of NU-1000**

NU-1000 was synthesized according to literature.<sup>3-5</sup> A 250-mL Pyrex media bottle was charged with  $\text{ZrOCl}_2 \cdot 8\text{H}_2\text{O}$  (0.392 g, 1.22 mmol), benzoic acid (8.000 g, 65.51 mmol), and DMF (32.0 mL). The mixture was heated in an oven at 100 °C for 1 h. After cooling to 23 °C,  $\text{H}_4\text{TBAPy}$  (0.160 g, 0.234 mmol) and TFA (160  $\mu\text{L}$ ) were added to the reaction mixture. Then the mixture was kept in the oven at 100 °C for 18 h. Yellow colored solids were collected and washed with DMF (7.0 mL  $\times$  3) and isolated by centrifuge. Furthermore, the solids were further washed by a mixture of 8 M HCl (1.0 mL) and DMF (48 mL) for 12 h at 100°C. The solids were continuously washed by hot DMF (7.0 mL  $\times$  3). The solids were soaked in acetone (5 mL  $\times$  3) to remove DMF. Finally, the solids were dried under reduced pressure to afford NU-1000 as yellow colored powder. Primary data is presented below: PXRD, Figures 2a and S1; SEM image, Figure S2,  $\text{N}_2$  adsorption isotherm at 77 K, Figure S3; Pore size distribution, Figure S4; IR, Figure S8.

### **Synthesis of NNO-2Ni-NU-1000(Zr) of different concentrations**

A 10-mL round bottom flask was charged with NU-1000 (0.100 g) and an ethanol solution (5.0 mL) of NNO-2Ni with a concentration of 0.025 M, 0.050 M, 0.075 M, 0.100 M, 0.150 M, or 0.200 M. The mixture was refluxed at 80 °C for 24 hours. The solids were collected and washed with additional ethanol. The MOF composite samples were obtained under reduced pressure at 80 °C.

### C. Supporting Data

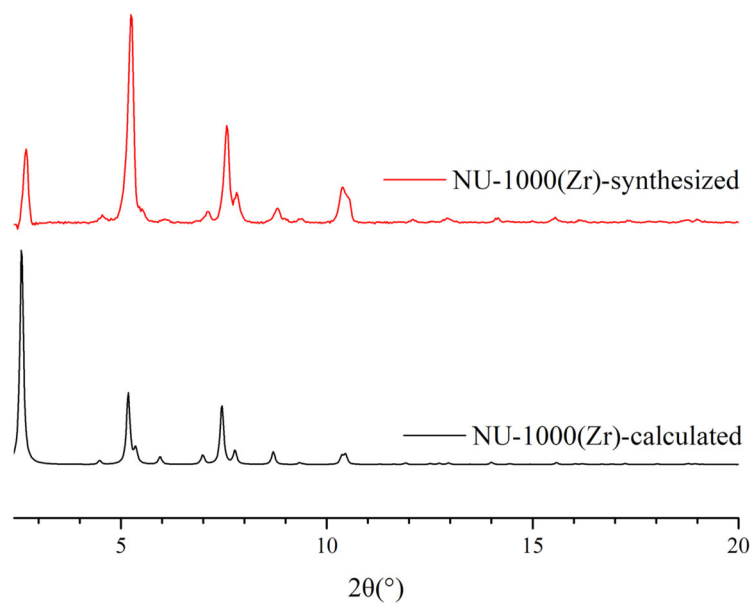


**Figure S1.** The experimental PXR D patterns of NU-1000 (—) are consistent with the calculated ones (—).

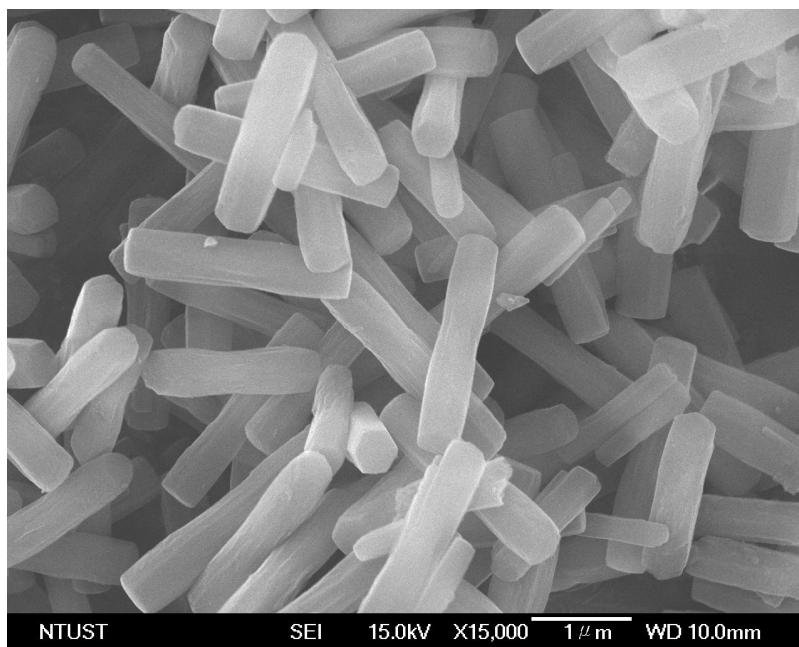


**Figure S2.** The SEM image of the obtained NU-1000 is presented to show the shape of crystals.

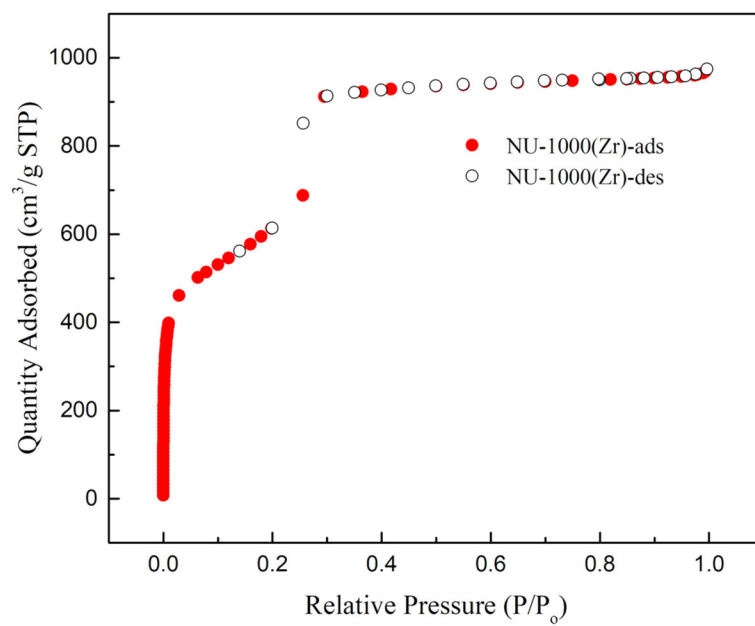


**Figure S3.** N<sub>2</sub> adsorption isotherm of NU-1000 was collected at 77 K.

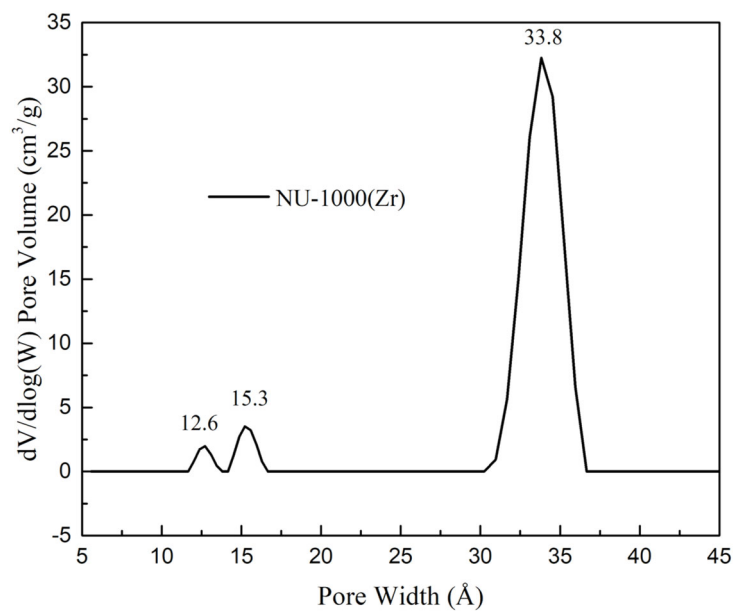


**Figure S4.** Pore size distribution of NU-1000 was calculated using the DFT model based on N<sub>2</sub> adsorption isotherm at 77 K.



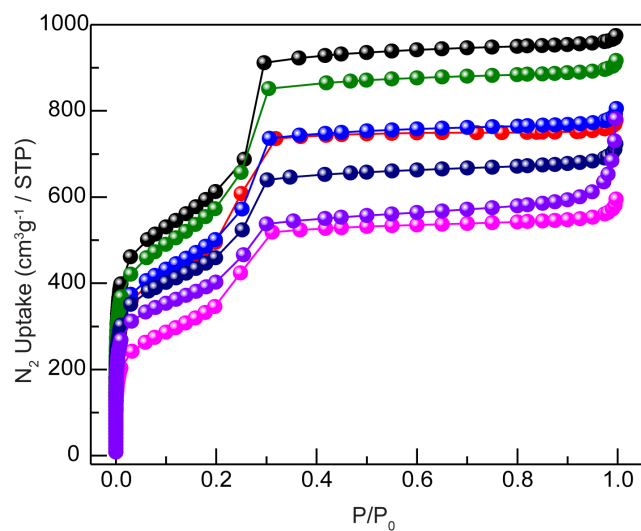


**Figure S5.** N<sub>2</sub> adsorption isotherms were collected on NU-1000 (●), NNO-2Ni-NU-1000 obtained by soaking NU-1000 in a range of NNO-2Ni EtOH solutions at different concentrations (NNO-2Ni(0.025)-NU-1000 (●), NNO-2Ni(0.050)-NU-1000 (●), NNO-2Ni(0.075)-NU-1000 (●), NNO-2Ni(0.100)-NU-1000 (●), NNO-2Ni(0.150)-NU-1000 (●), and NNO-2Ni(0.200)-NU-1000 (●)).

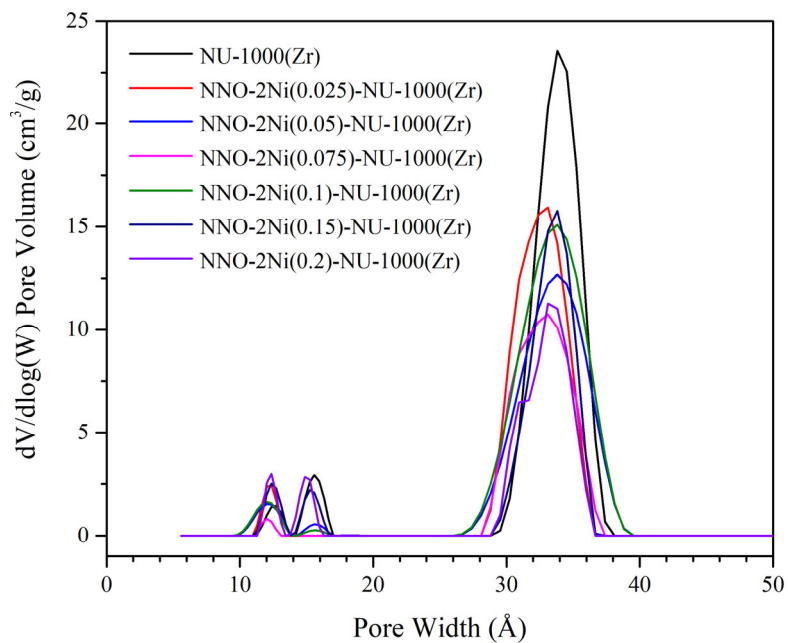


**Figure S6.** Pore size distribution plots of NNO-2Ni-NU-1000 were calculated using the DFT model based on  $\text{N}_2$  adsorption isotherms at 77 K.

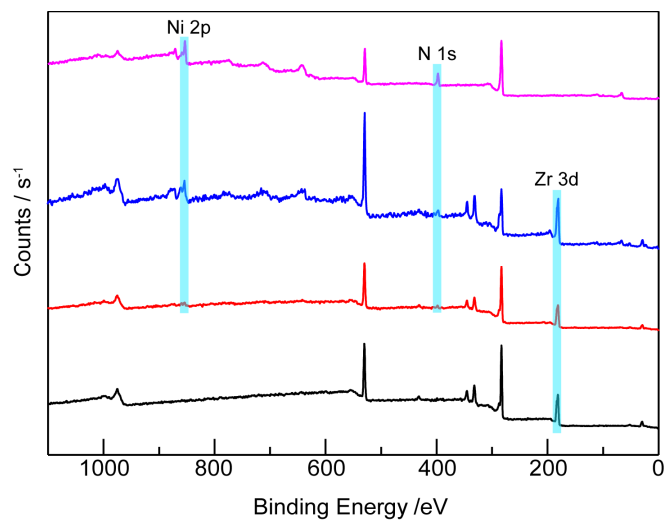


**Figure S7.** The X-ray photoelectron spectra were conducted on NU-1000 (—), NNO-2Ni(0.050)-NU-1000 (—), and NNO-2Ni(0.100)-NU-1000 (—), and NNO-2Ni (—).

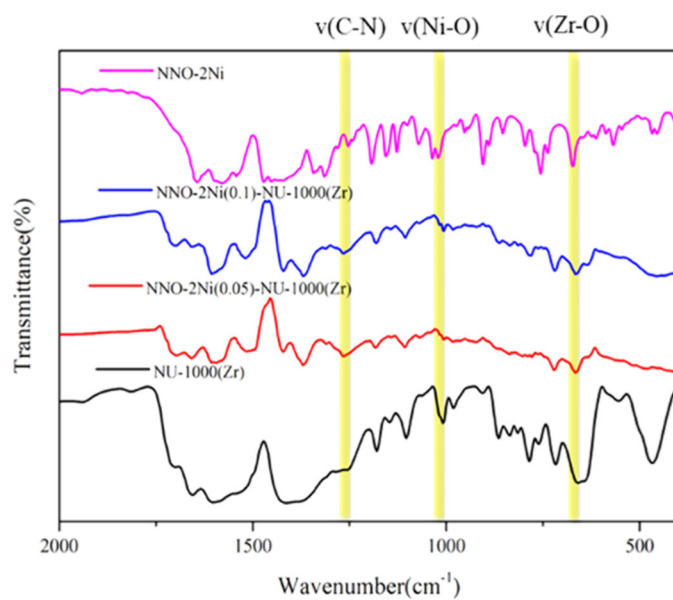


**Figure S8.** IR spectra (2000–450  $\text{cm}^{-1}$ ) were collected from NU-1000 (—), NNO-2Ni(0.05)-NU-1000 (—), NNO-2Ni(0.100)-NU-1000 (—), and NNO-2Ni (—).

### Utilizing ICP-OES to determine Ni content in NNO-2Ni-NU-1000

The ICP-OES data reveals that 50 mg of NNO-2Ni(0.050)-NU-1000 contains 1.25 mg of Ni metal, while 50 mg of NNO-2Ni(0.100)-NU-1000 contains 1.02 mg of Ni metal. The following calculation converts this information into the amount of the molecular complex, NNO-2Ni, per MOF unit,  $[\text{Zr}_6(\mu_3\text{-O})_4(\mu_3\text{-OH})_4(\text{H}_2\text{O})_4(\text{OH})_4(\text{TBAPy})_2]$ .

$$m_{\text{Ni}}(\%) = \frac{(n_{2\text{Ni}}) \times (2) \times (58.69)}{M_{\text{sample}}}$$

$$M_{\text{sample}} = 2176.76 + n_{2\text{Ni}} \times (636.00)$$

Within the equations,  $m_{\text{Ni}}(\%)$  represents the weight percentage of Ni in the MOF composite,  $n_{2\text{Ni}}$  represents the moles of the molecular complex, NNO-2Ni, and  $M_{\text{sample}}$  indicates the formula weight of the MOF composite.

Solving the above equations for  $n_{2\text{Ni}}$ , the values are  $n_{2\text{Ni}(0.050)} = 0.54$  and  $n_{2\text{Ni}(0.100)} = 0.43$ .

**Table S1.** Determination of Ni content in NNO-2Ni-NU-1000 using ICP-OES data.

Sample	Ni Mass / mg	Sample Mass / mg	$n_{2\text{Ni}}$
NU-1000(Zr)	Not detected (ND)	50	None
NNO-2Ni(0.050)-NU-1000	1.25	50	0.54
NNO-2Ni(0.100)-NU-1000	1.02	50	0.43

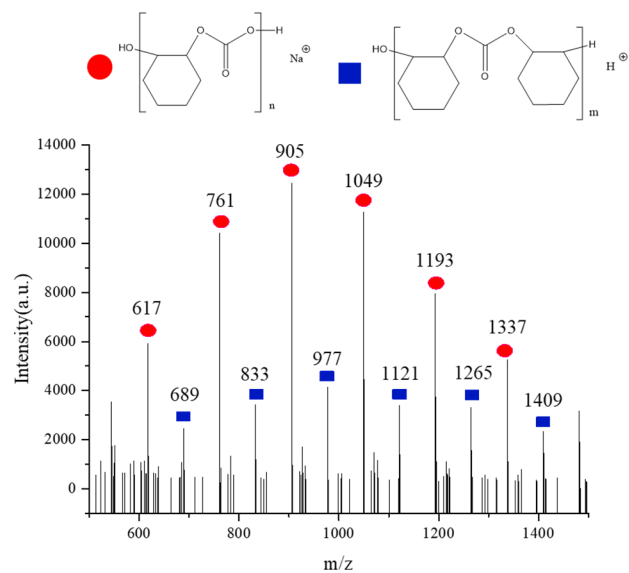
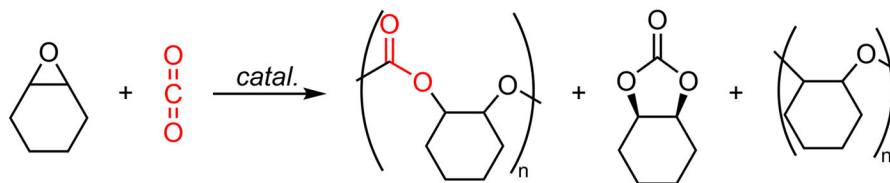


**Figure S9.** The MALDI-TOF mass spectrum for poly(cyclohexene carbonate) was obtained from Table 1, Entry 6.

**Table S2.** Catalytic performances of NNO-2Ni(0.050)-NU-1000 at different TBAT (the co-catalyst) loadings are presented.



Entry	TBAB /mmol%	CHO conv. / % <sup>a</sup>	CHC / % <sup>a</sup>	Polymer / % (PCHC / %) <sup>a</sup>	Mn (Đ) <sup>b</sup>
1	0.50	> 99	>99	<1	NA
2	0.25	96	>99	<1	NA
3	0.10	94	75	25 (> 99)	430 (1.17)

The reaction was carried out using 35 mmol cyclohexene oxide in the presence of NNO-2Ni(0.050)-NU-1000 (50 mg) and TBAB under the initial CO<sub>2</sub> pressure of 300 psi for 24 h at 100 °C with a stir rate of 100 rpm.

<sup>a</sup> These results were analyzed by peak shift in <sup>1</sup>H NMR spectra collected in a mixture of CDCl<sub>3</sub> and C<sub>6</sub>D<sub>6</sub> (v/v= 1/4.5). The characteristic peaks include δ at 4.65 ppm for PCHC, δ at 3.45 ppm for undesired polymer with ether linkage, δ at 3.20 ppm *trans*-CHC, and δ at 3.80 ppm for *cis*-CHC.

<sup>b</sup> Evaluated via GPC using THF as the eluent and calibrated against narrow molecular weight polystyrene standards.

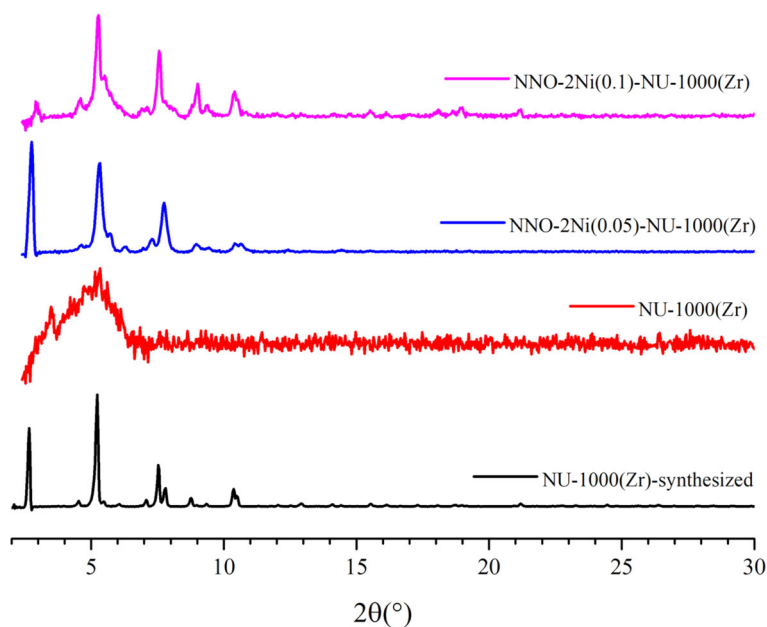


**Figure S10.** The catalytic reactions between CHO and CO<sub>2</sub> were carried out by different catalysts (Entries 1-3, Table 1). PXRD patterns were collected from post-catalysis samples, including NU-1000 (—), NNO-2Ni(0.050)-NU-1000 (—), and NNO-2Ni(0.100)-NU-1000 (—). Compared to the as-synthesized NU-1000 before catalysis (—), the MOF composites having NNO-2Ni complexes in the lattice show improved crystallinity after the catalysis.



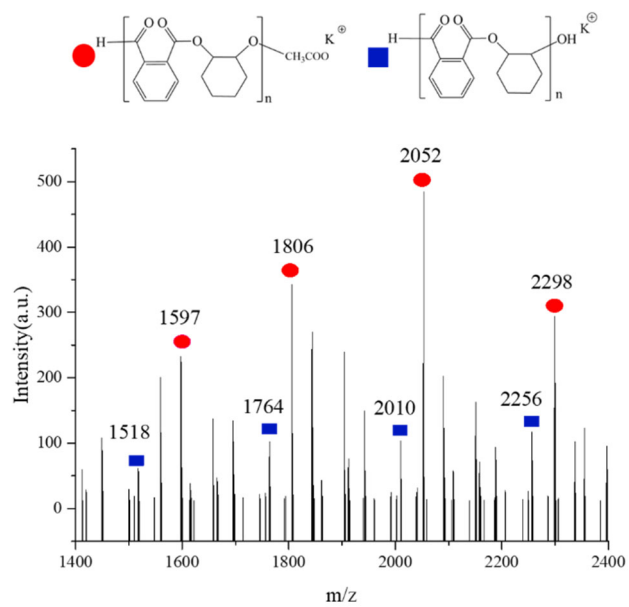
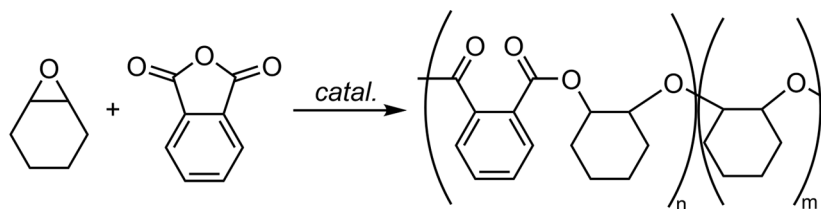


**Figure S11.** The MALDI-TOF mass spectrum for poly (PA-alt-CHO) obtained from Table 3, Entry 3.

**Table S3.** The spent NNO-2Ni(0.050)-NU-1000 was tested four more time toward the copolymerization of CHO and PA.



Entry	PA conv. /% <sup>a</sup>	CHO conv. /% <sup>a</sup>	Ester : Ether <sup>b</sup>	Mn ( <i>D</i> ) <sup>c</sup>
1	84	>99	30:70	700 (1.23)
2	80	>99	30:70	2100 (1.31)
3	84	>99	30:70	2800 (1.36)
4	80	>99	30:70	2800 (1.37)

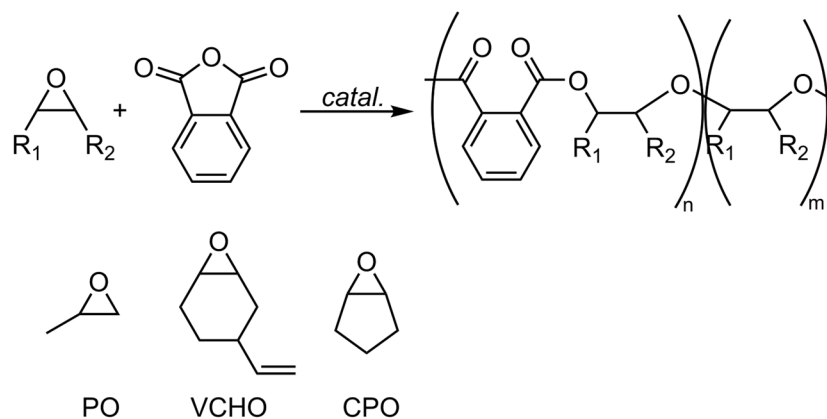
The copolymerization reactions were carried out using 35 mmol CHO, 35 mmol PA in toluene (1.0 mL) in the presence of collected NNO-2Ni(0.050)-NU-1000 (100 mg) as the catalyst and 9-AnOH (2.0 mol%) as the chain transfer agent. The reaction was kept at 110 °C for 24 h with a stir rate of 400 rpm.

<sup>a</sup> These results were analyzed by comparing integrals of PA (7.97 ppm) and aromatic signals of PE (7.30-7.83 ppm) in the <sup>1</sup>H NMR spectrum collected in CDCl<sub>3</sub>.

<sup>b</sup> The ratios of ester/ether were calculated based on integrals of ester (4.80–5.26 ppm) and ether (3.22–3.64 ppm) in the <sup>1</sup>H NMR spectrum collected in CDCl<sub>3</sub>.

<sup>c</sup> Evaluated via GPC using THF as the eluent and calibrated against narrow molecular weight polystyrene standards.

**Table S4.** The scope of epoxide was expanded to include PO, VCHO, and CPO during its copolymerization with PA.



Entry	Epoxide	PA conv. / % <sup>a</sup>	Epoxide conv. / % <sup>a</sup>	Ester : Ether <sup>b</sup>	Mn ( $\bar{D}$ ) <sup>c</sup>
1	PO	80	85	23:77	2000 (1.10)
2	VCHO	80	86	72:28	1350 (1.30)
3	CPO	67	70	43:57	970 (1.22)

The copolymerization reactions were carried out using 35 mmol epoxide, 35 mmol PA in toluene (1.0 mL) in the presence of NNO-2Ni(0.050)-NU-1000 (100 mg) as the catalyst and 9-AnOH (2.0 mol%) as the chain transfer agent. The reaction was kept at 110 °C for 24 h with a stir rate of 400 rpm.

<sup>a</sup> These results were analyzed by comparing integrals of PA (7.97 ppm) and aromatic signals of PE (7.30-7.83 ppm) in the <sup>1</sup>H NMR spectrum collected in CDCl<sub>3</sub>.

<sup>b</sup> The ratios of ester/ether were calculated based on integrals of ester (4.80–5.26 ppm) and ether (3.22–3.64 ppm) in the <sup>1</sup>H NMR spectrum collected in CDCl<sub>3</sub>.

<sup>c</sup> Evaluated via GPC using THF as the eluent and calibrated against narrow molecular weight polystyrene standards.

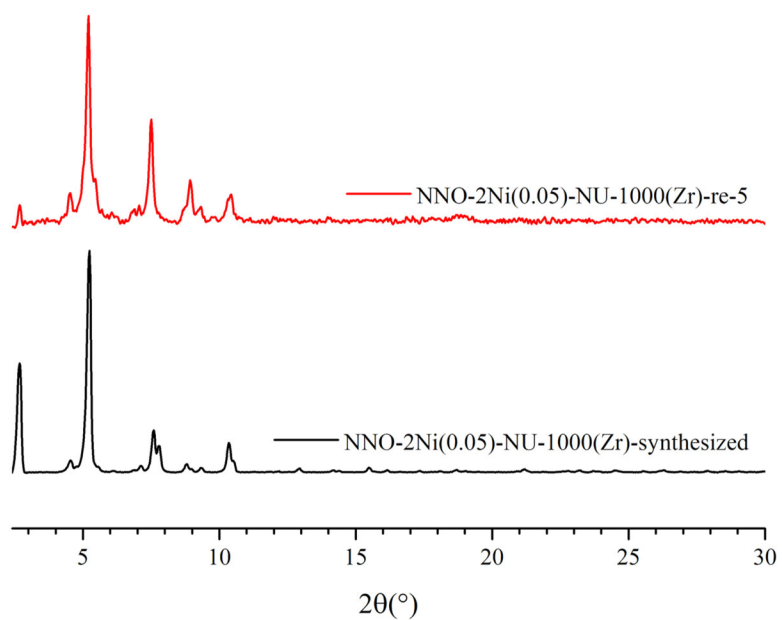


**Figure S12.** PXRD patterns collected from the solvothermally synthesized and activated NNO-2Ni(0.050)-NU-1000 before catalysis (—), NNO-2Ni(0.050)-NU-1000(Zr) after 5 catalytic cycles (—).

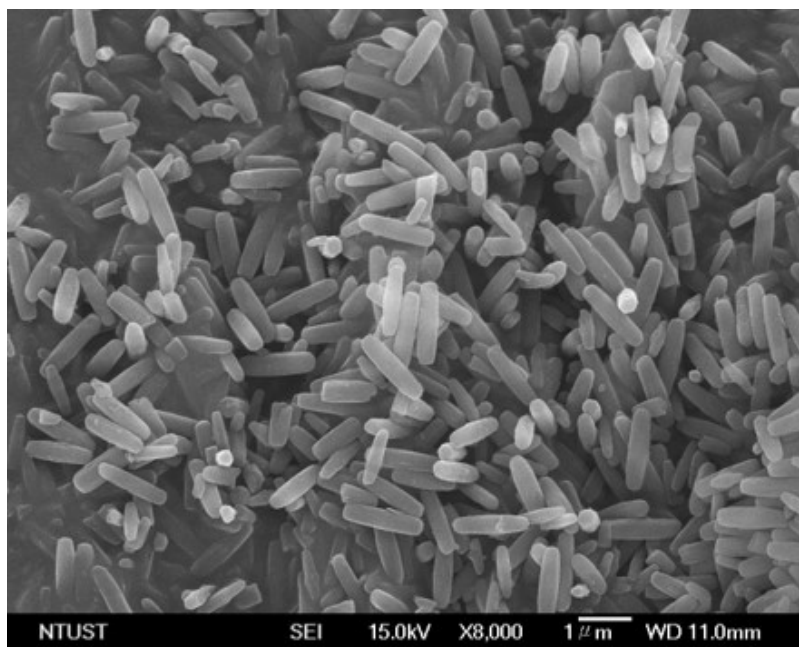


**Figure S13.** The SEM image of the NNO-2Ni(0.050)-NU-1000(Zr) after 5 catalytic cycles is presented to show the shape of crystals.

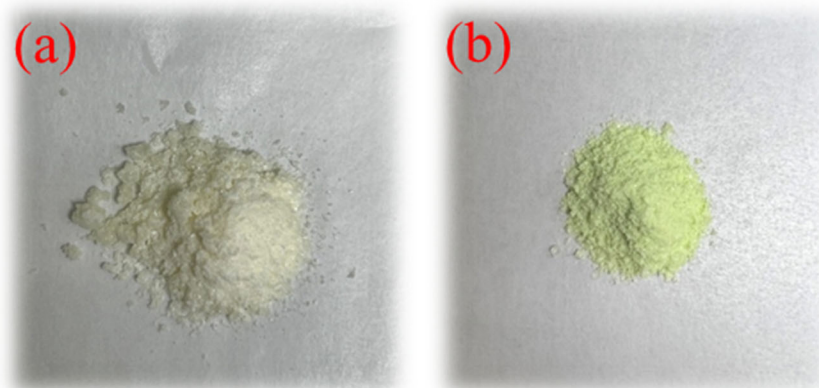


**Figure S14.** (a) The copolymer was obtained using NNO-2Ni(0.050)-NU-1000 as the catalyst from Table 3, Entry 1. (b) The copolymer was obtained using the homogeneous NNO-2Ni molecular catalyst. Polymers catalyzed by the homogeneous catalyst often exhibit intense metal-derived coloration, necessitating an acid-washing step for decolorization after the reaction or removal of the nickel residue. However, polymers obtained using the MOF-based heterogeneous catalyst retain the color like that of the pristine polymer, thereby reducing the need for extensive post-treatment.

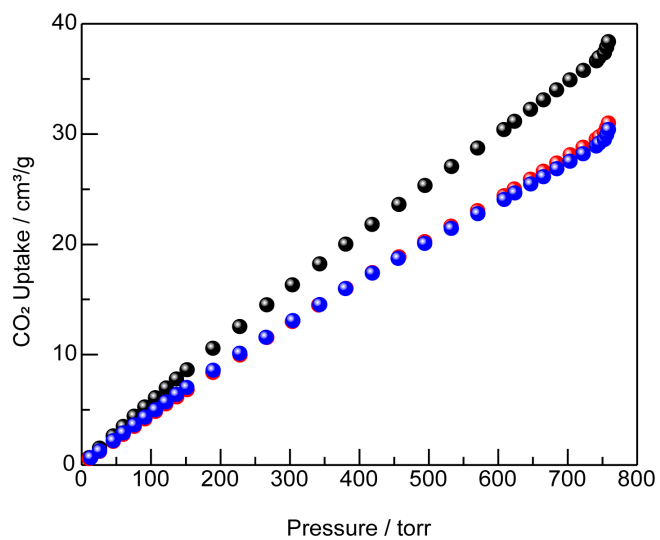


**Figure S15.** CO<sub>2</sub> adsorption isotherms were collected on NU-1000 (●), NNO-2Ni(0.050)-NU-1000 (●), and NNO-2Ni(0.100)-NU-1000(●) at 298 K. These experimental results indicate that the incorporation of NNO-2Ni did not enhance CO<sub>2</sub> adsorption capacity.

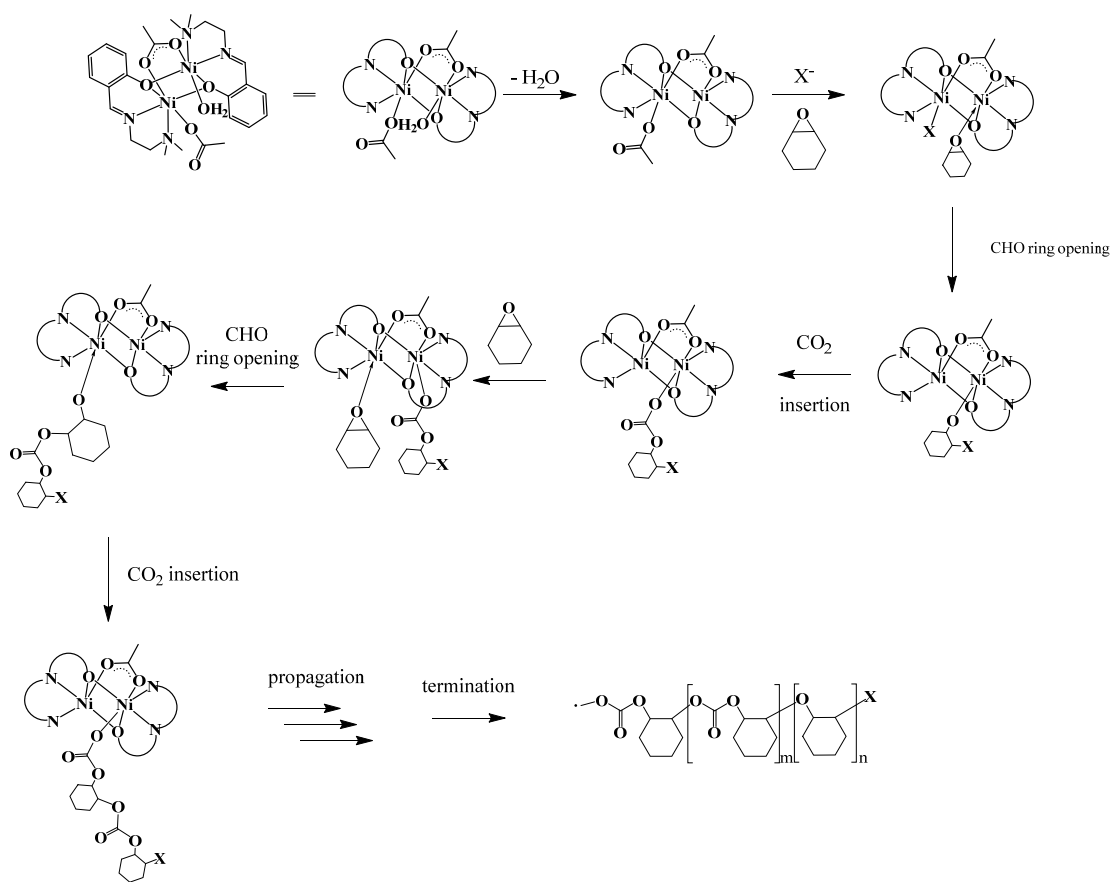


**Figure S16.** A tentative mechanism for the copolymerization of CHC and CO<sub>2</sub> is presented. NU-1000 is unable to catalyze this copolymerization reaction presented as the control experiment as Table 1, Entry 1, which only produces the cyclohexene carbonate. This suggests that the active site responsible for the copolymerization reaction is the Ni center in NNO-2Ni. In the first step, H<sub>2</sub>O dissociates from the metal center, creating an open coordination site. Subsequently, CHO coordinates with the metal center. The initiator on another Ni metal facilitates the ring-opening of CHO, followed by CO<sub>2</sub> insertion. After the propagation reaction, the polymer chain continues to grow. Finally, the polymer is obtained through the termination reaction.<sup>6, 7</sup>



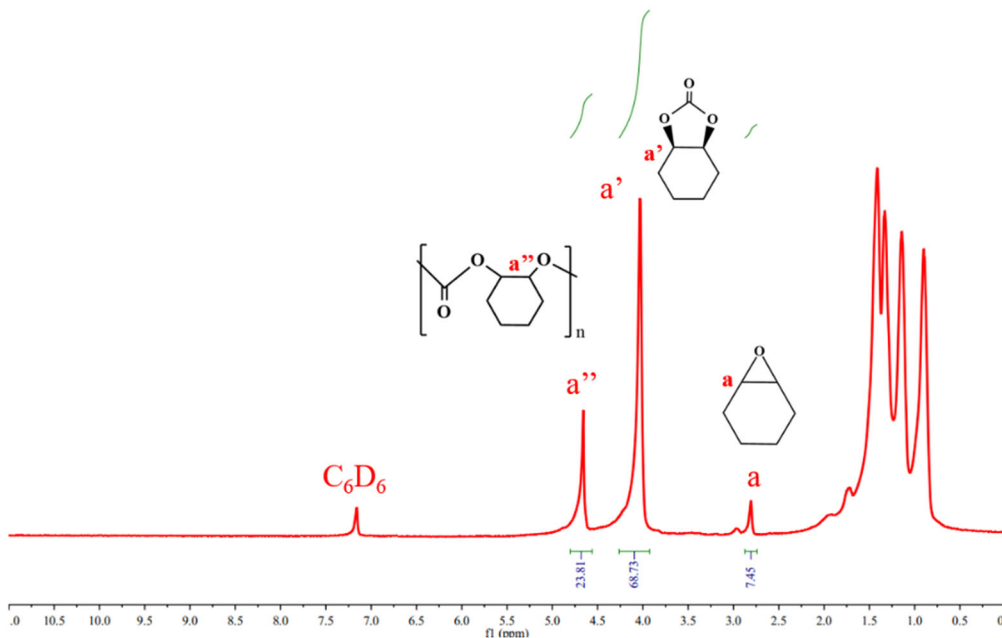


**Figure S17.** The  $^1\text{H}$  NMR spectrum was acquired in a mixture of  $\text{CDCl}_3$  and  $\text{C}_6\text{D}_6$  (v/v = 1 : 4.5) for the reaction between  $\text{CHO}$  and  $\text{CO}_2$ , listed as Entry 2, Table 1.

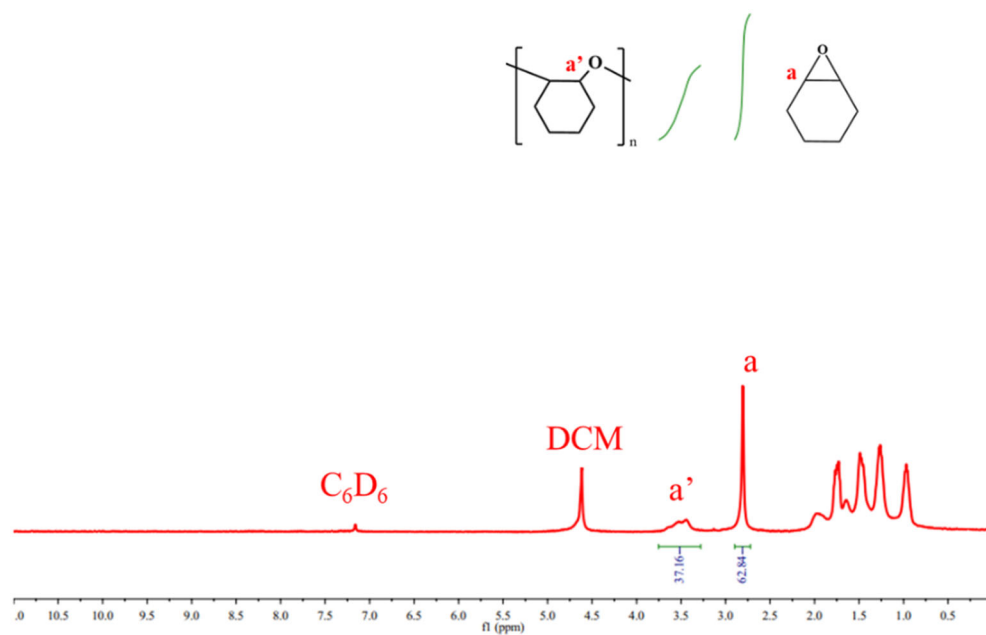


**Figure S18.** The  $^1\text{H}$  NMR spectrum was acquired in a mixture of  $\text{CDCl}_3$  and  $\text{C}_6\text{D}_6$  (v/v = 1 : 4.5) for Entry 7, Table 1.

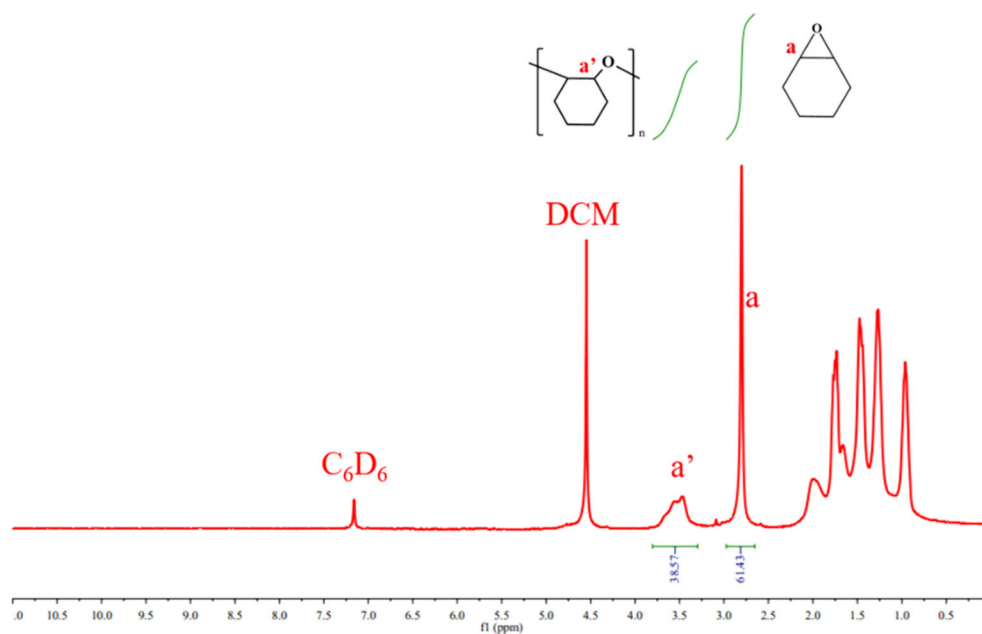


**Figure S19.** The  $^1\text{H}$  NMR spectrum was acquired in a mixture of  $\text{CDCl}_3$  and  $\text{C}_6\text{D}_6$  (v/v = 1 : 4.5) for Entry 8, Table 1.

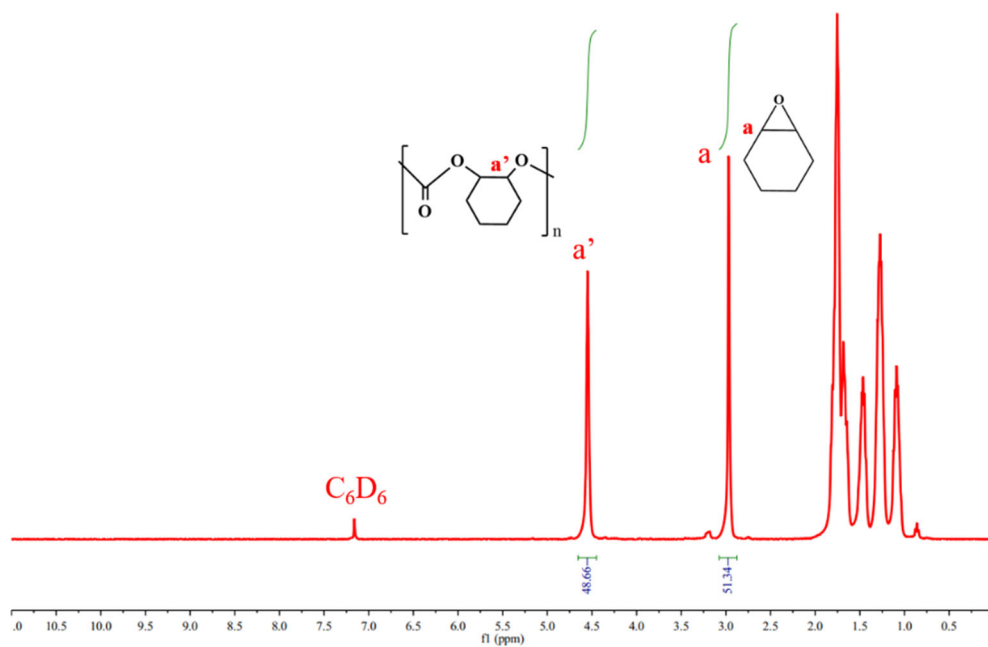


**Figure S20.** The  $^1\text{H}$  NMR spectrum was acquired in a mixture of  $\text{CDCl}_3$  and  $\text{C}_6\text{D}_6$  (v/v = 1 : 4.5) for Entry 2, Table 2.

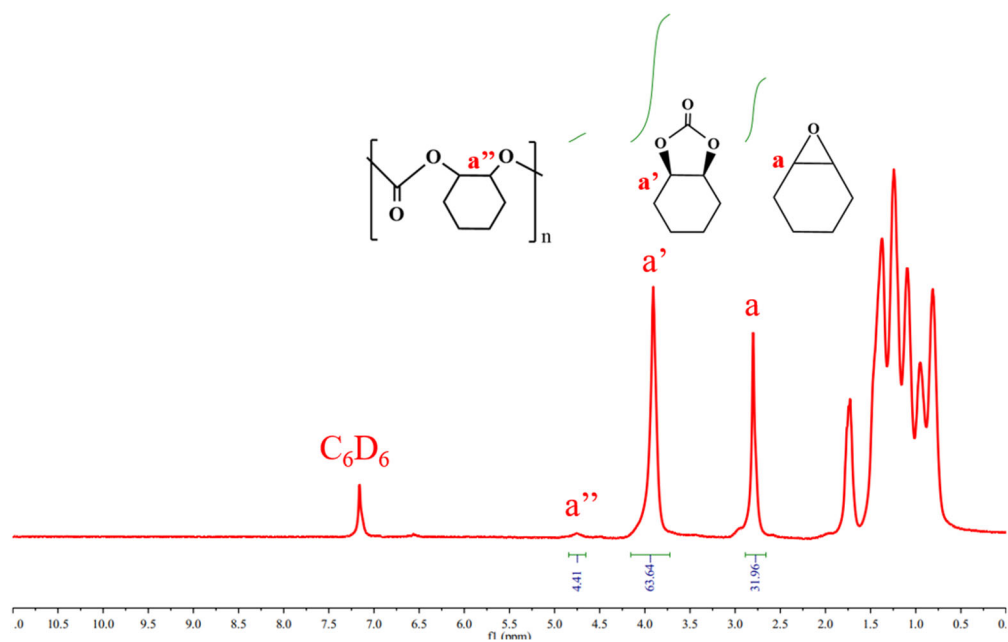


**Figure S21.** The  $^1\text{H}$  NMR spectrum was acquired in a mixture of  $\text{CDCl}_3$  and  $\text{C}_6\text{D}_6$  (v/v = 1 : 4.5) for Entry 3, Table 2.

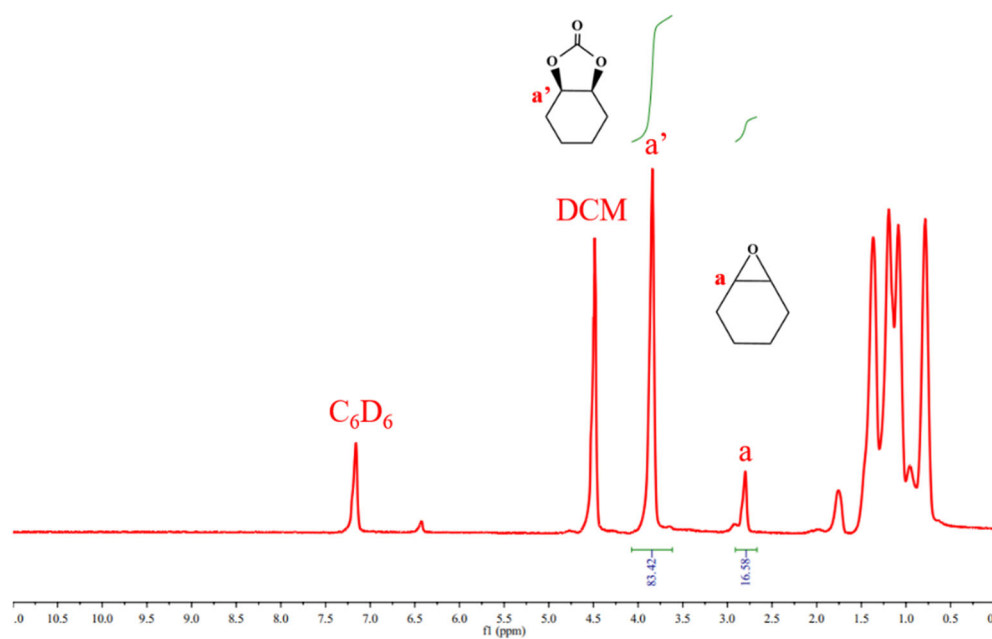


**Figure S22.** The  $^1\text{H}$  NMR spectrum was acquired in a mixture of  $\text{CDCl}_3$  and  $\text{C}_6\text{D}_6$  (v/v = 1 : 4.5 with DCM) for Entry 4, Table 2.

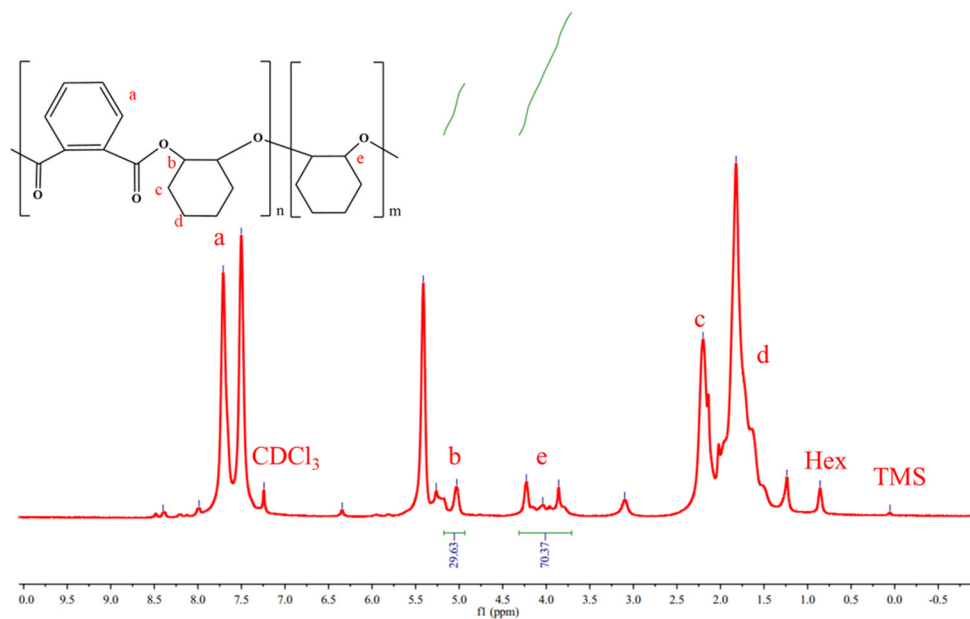


**Figure S23.** The <sup>1</sup>H NMR spectrum was acquired in CDCl<sub>3</sub> the copolymerization of PA and CHO, listed as Entry 1, Table 3.

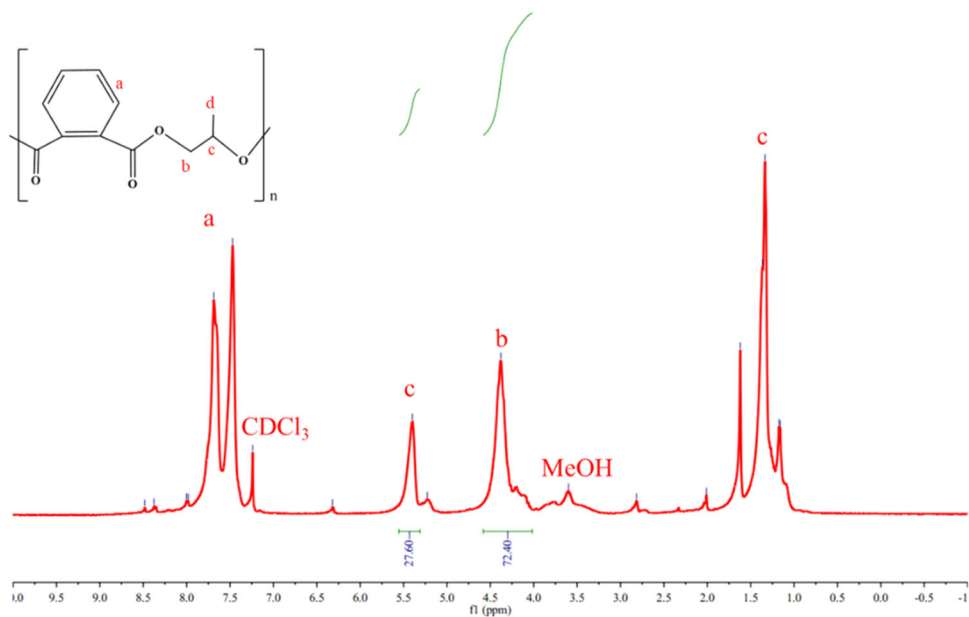


**Figure S24.** The <sup>1</sup>H NMR spectrum was acquired in CDCl<sub>3</sub> the copolymerization of PA and PO, listed as Entry 1, Table S4.



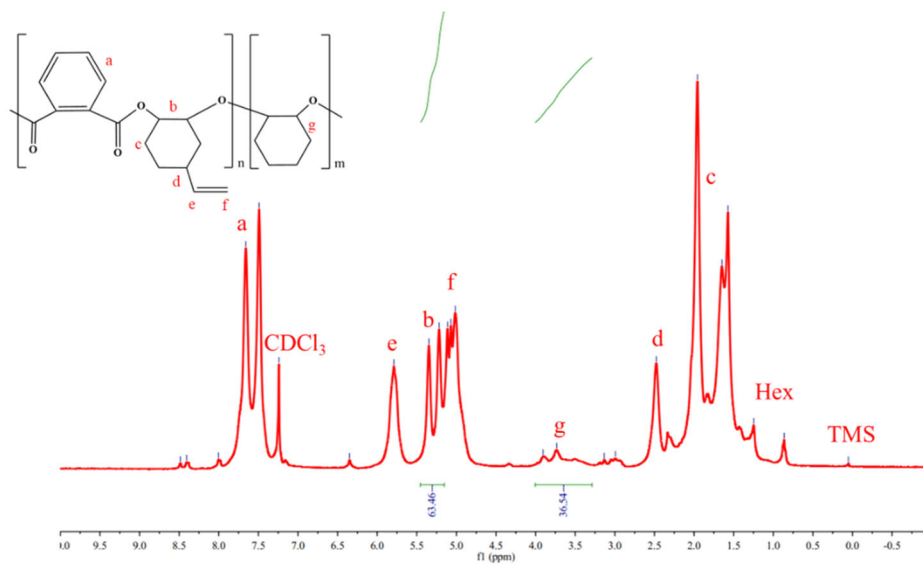


**Figure S25.** The <sup>1</sup>H NMR spectrum was acquired in CDCl<sub>3</sub> the copolymerization of PA and VCHO, listed as Entry 2, Table S4.

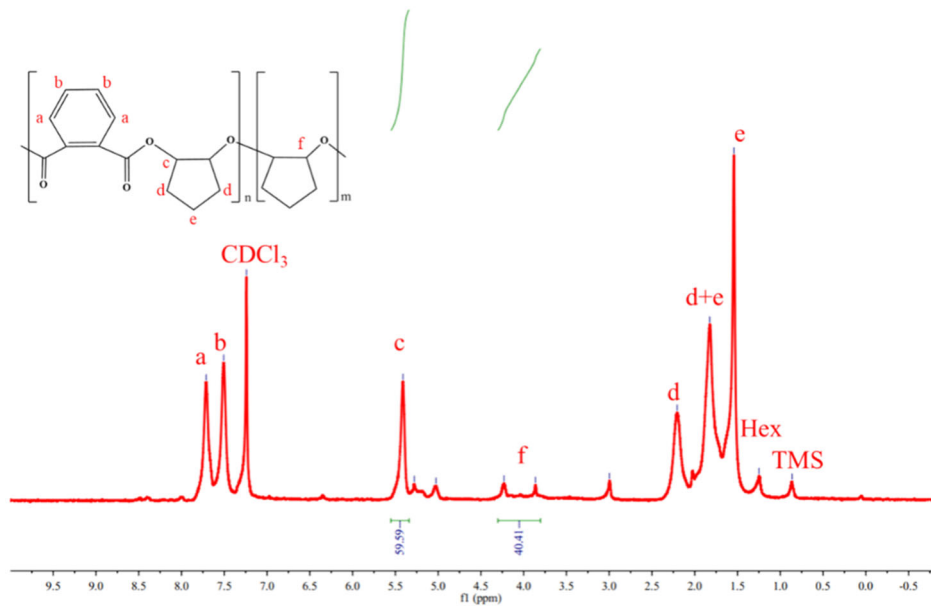


**Figure S26.** The <sup>1</sup>H NMR spectrum was acquired in CDCl<sub>3</sub> the copolymerization of PA and CPO, listed as Entry 3, Table S4.

## D. References

1. Tsai, C.-Y.; Cheng, F.-Y.; Lu, K.-Y.; Wu, J.-T.; Huang, B.-H.; Chen, W.-A.; Lin, C.-C.; Ko, B.-T., Dinuclear and Trinuclear Nickel Complexes as Effective Catalysts for Alternating Copolymerization on Carbon Dioxide and Cyclohexene Oxide. *Inorg. Chem.* **2016**, *55* (16), 7843-51.
2. Fulmer, G. R.; Miller, A. J. M.; Sherden, N. H.; Gottlieb, H. E.; Nudelman, A.; Stoltz, B. M.; Bercaw, J. E.; Goldberg, K. I., NMR Chemical Shifts of Trace Impurities: Common Laboratory Solvents, Organics, and Gases in Deuterated Solvents Relevant to the Organometallic Chemist. *Organometallics* **2010**, *29* (9), 2176-2179.
3. Islamoglu, T.; Otake, K.-i.; Li, P.; Buru, C. T.; Peters, A. W.; Akpınar, I.; Garibay, S. J.; Farha, O. K., Revisiting the structural homogeneity of NU-1000, a Zr-based metal-organic framework. *CrystEngComm* **2018**, *20* (39), 5913-5918.
4. Webber, T. E.; Desai, S. P.; Combs, R. L.; Bingham, S.; Lu, C. C.; Penn, R. L., Size Control of the MOF NU-1000 through Manipulation of the Modulator/Linker Competition. *Cryst. Growth Des.* **2020**, *20* (5), 2965-2972.
5. Syed, Z. H.; Mian, M. R.; Patel, R.; Xie, H.; Pengmei, Z.; Chen, Z.; Son, F. A.; Goetjen, T. A.; Chapovetsky, A.; Fahy, K. M.; Sha, F.; Wang, X.; Alayoglu, S.; Kaphan, D. M.; Chapman, K. W.; Neurock, M.; Gagliardi, L.; Delferro, M.; Farha, O. K., Sulfated Zirconium Metal-Organic Frameworks as Well-Defined Supports for Enhancing Organometallic Catalysis. *J. Am. Chem. Soc.* **2022**, *144* (37), 16883-16897.
6. Su, Y.-C.; Ko, B.-T., Alternating Copolymerization of Carbon Dioxide with Epoxides Using Highly Active Dinuclear Nickel Complexes: Catalysis and Kinetics. *Inorg. Chem.* **2021**, *60* (2), 852-865.
7. Su, Y.-C.; Liu, G.-L.; Ko, B.-T., Bimetallic Nickel Complexes as Effective and Versatile Catalysts for Copolymerization of Epoxides with Carbon Dioxide or Phthalic Anhydride: Catalysis and Kinetics. *Inorg. Chem.* **2023**, *62* (22), 8565-8575.